On the Formation of Centreline Segregation in Continuous Slab Casting of Steel due to Bulging and/or Feeding

F. Mayer*, M. Wu, and A. Ludwig

Christian Doppler Laboratory for Multiphase Modeling of Metallurgical Processes, Department Metallurgy, University of Leoben, A-8700 Leoben, Austria

* Corresponding author; e-mail: florian.mayer@unileoben.ac.at

Centreline macrosegregation is often observed in continuous slab casting of steel. Two of the main macrosegregation formation mechanisms are bulging and feeding. Both were studied and compared in the current work by using a two-phase volume averaging model considering only columnar solidification. The casting of the strand itself is modelled by applying a predefined velocity following the casting speed and solid shell deformation (e.g. bulging). Three different cases are simulated and discussed. (i) The first case considers the influence of the feeding flow during solidification without taking bulging into account. Negative macrosegregation is observed in the centre of the casting in this case. (ii) The second case takes the flow caused by series of bulging along the solidifying strand shell into account, and is, therefore, representative for an ideal situation where bulging takes place without solidification shrinkage. In this case positive centreline segregation is found. (iii) The last case shows the results of a simulation which combines both shrinkage- and bulging-induced flows. It is found that under the current casting conditions the bulging effect dominates over the shrinkage effect, and so positive centreline segregation is predicted.

Keywords: macrosegregation, slab casting, bulging, centreline segregation, feeding flow, softreduction, modelling

Submitted on 13 March 2010, Accepted on 20 May 2010

Introduction

Industrial practice has shown that the typical centreline segregation in continuous slab casting of steel can be reduced by the so-called soft reduction at/near the end of solidification [1–8]. Gaining deeper knowledge about the formation mechanism of centreline macrosegregation and the effectiveness of soft reduction based on experimental trials is exhausting and costly. Therefore, detailed numerical studies become more and more important to achieve improved understanding on this production process [9–13].

The current authors [14–16] have developed a volume-averaging-based solidification model for predicting macrosegregation. This approach can consider the melt flow caused by shrinkage and thermo-solutal buoyancy, the motion of equiaxed crystals, the progress of a columnar front and the columnar-to-equiaxed transition. In the present paper two phases, columnar dendrite drunks and the interdendritic melt, are taken into account. The mechanical deformation of the solid shell, i.e. bulging, is modelled according to a predefined geometry. No mechanical deformation model is considered. The idea to describe the velocity of the solidified shell due to bulging as proposed by Miyazawa and Schwerdtfeger [9], is employed and modified. As the aim of this work is to improve understanding on the formation of centreline macrosegregation a benchmark casting (simplified 2D steel slab with series of bulging) is simulated. With such a model the idea to reduce/minimize centreline segregation by soft reduction can be numerically investigated.

Model

Two phase solidification model. Details of the numerical model for columnar solidification are described previously [14–16, 18, 19]. In general, it has to be stated that the two phases considered in the current model are melt and columnar dendrite trunks. The columnar phase is considered to have cylindrical morphology growing from the mould wall with constant primary dendrite arm spacing, λ_1. A volume-average model is applied. The volume-averaged concentrations (c_ℓ, c_s) are considered to be different from the concentrations at the liquid-solid interface (c_ℓ^*, c_s^*) which are determined according to equilibrium thermodynamics. The difference ($c_\ell^* - c_\ell$) serves as driving force for the growth of the columnar trunks. Macrosegregation is calculated by the mixture concentration $c_{mix} = (\rho_\ell c_\ell f_\ell + \rho_s c_s f_s)/(\rho_\ell f_\ell + \rho_s f_s)$.

Solid back diffusion is not considered in the current work. The thermodynamics of a linearized binary Fe-C phase diagram is taken into account by using a constant solute partitioning coefficient k and liquidus slope m. Hydrodynamic interaction between solid and liquid in the mushy zone is calculated via a permeability law according to the Blake-Kozeny approach. For modelling of solidification shrinkage deep in the mushy zone the so-called 'simplified porosity model (SPM)' [18, 19] is used when the local solid volume fraction exceeds a critical point, $f_{s,SPM}$. Beyond $f_{s,SPM}$ the permeability of the dendritic region is sufficient low that no relative velocity between the interdendritic melt and the solid dendrites occurs. Therefore, the rest melt is supposed to solidify with the same density as the

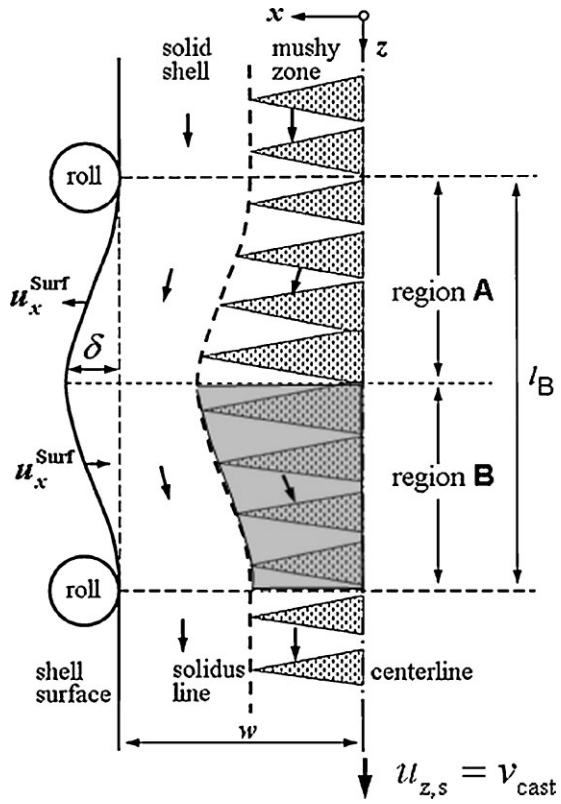

Figure 1. Schematic of solid motion between one pair of bulging rolls; reproduced from [9].

melt. It implies that the rest melt deep in the mushy zone solidifies with 'mini pores' being frozen in the interdendritic region.

Motion of the solid in the mushy zone. Miyazawa and Schwerdtfeger proposed a solid velocity field in the mushy region between two neighbouring rolls [9]. As schematically shown in **Figure 1**, the z-component of solid velocity, u_z, is assumed to be constant, i.e. casting speed. (The correct symbol for the z-component of solid velocity should be $u_{z,s}$, where the subscript s indicates the solid phase. For simplicity, however, this paper uses u_z to represent the solid velocity in z-component). For the totally solidified strand shell the x-component of solid velocity, u_x, is assumed to be equal to the surface velocity, u_x^{Surf}. The surface velocity of the strand shell can be derived according to the predefined bulging profile of the geometry. With the above assumptions the continuity condition of the fully-solidified domain is fulfilled: $\partial u_z/\partial z + \partial u_x/\partial x = 0$. In the mushy zone, two regions are distinguished: A and B. In the region A where the strand thickens due to bulging, the solid velocity x-component, u_x, is supposed to be constant and equal to surface velocity of the shell, u_x^{Surf}. In the region B where the strand is pressed together, u_x is supposed to be linearly reduced from the maximum in the complete solid region to zero at the casting centre

$$u_x = u_x^{\mathrm{Surf}} \cdot \frac{f_s - f_s^{\mathrm{cent}}}{1 - f_s^{\mathrm{cent}}}, \tag{1}$$

with f_s^{cent} being the solid volume fraction at the casting centre. This linear velocity reduction mimics deformation within the partly solid strand.

In the present paper the above outlined idea from [9] is employed with necessarily extensions to consider multiple bulging rolls, as shown in **Figure 2**. The z-component of solid velocity, u_z, is still considered as constant, i.e. casting speed. For the x-component of the solid velocity, u_x, more sophisticated situations must be considered. For regions where the dendrite tips, approximated by the liquidus front, have not met the casting centreline, we still assume that the solid dendrites move with the same velocity as that of the fully solidified strand shell. Only when the temperature of the casting centreline drops below the liquidus temperature of the corresponding segregated melt near the centreline, two regions are distinguished: A and B. (see 'non-strength core' zone in Figure 2). Similarly, in the region A, the solid velocity x-component, u_x, is set to be constant and equal to surface velocity of the shell, u_x^{Surf}. In the region B, u_x is supposed to be reduced from its maximum at a position of solid fraction $f_s^{0-\mathrm{strength}}$ to zero at the casting centre. We believe that it is more likely that deformations happen at the dendritic strand core where the solid volume fraction is smaller than the so-called "0-strength" volume fraction $f_s^{0-\mathrm{strength}}$ rather than across the whole section of the mushy zone. According to industrial experiences $f_s^{0-\mathrm{strength}} = 0.8$

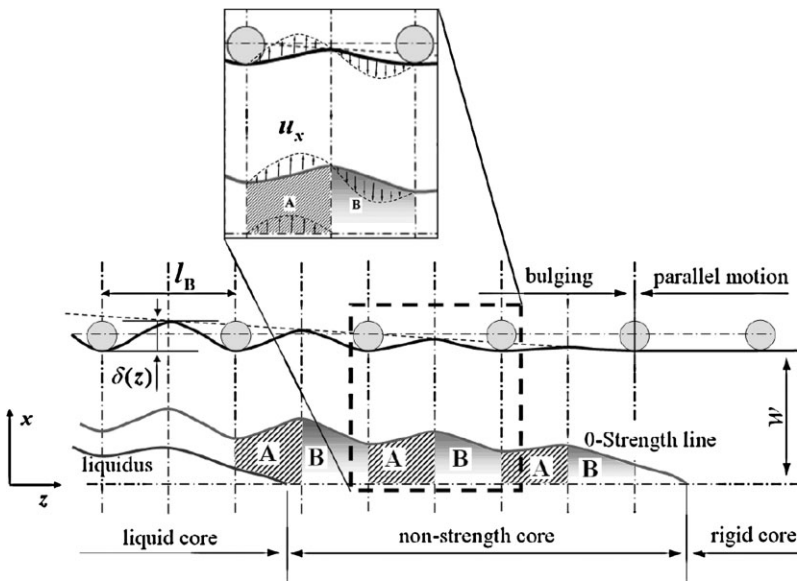

Figure 2. Schematic of solid motion with a series of bulging rolls.

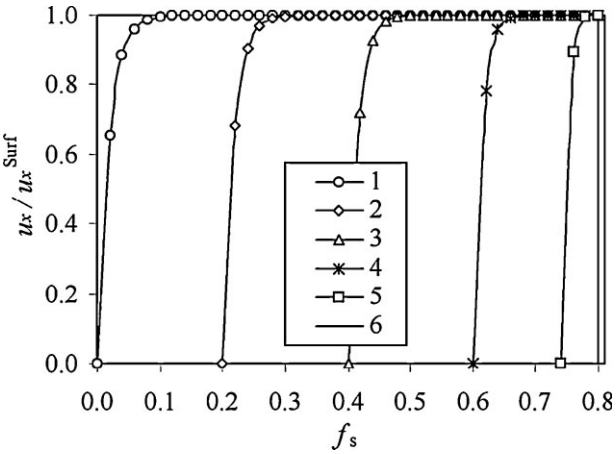

Figure 3. Normalized velocity profiles for different solid volume fractions according to Equation (2). Lines 1–5 exemplarily show the evolution of the normalized velocity for 5 different values of f_s^{cent}: 0.0, 0.2, 0.4, 0.6, 0.74 correspondingly. Line 6 shows the position of 0-strength at $f_s = 0.8$.

has been chosen in the present work. The following modification of Equation (1) is suggested

$$u_x = u_x^{Surf} \cdot \left(1 - e^{-k \cdot \frac{(f_s - f_s^{cent})}{(f_s^{0-strength} - f_s)^n}}\right) \quad (2)$$

where the constants $k = 50$ and $n = 0.25$ were chosen to ensure a smooth transition. Equation (2) leads to normalized velocity profiles as displayed in **Figure 3** exemplarily for 5 different f_s^{cent}.

In order to implement the above idea into the two phase solidification model, the z component of the solid velocity, u_z, is set to the casting velocity for the whole calculation domain, whereas for the x-component of the solid velocity, u_x, the strand is divided into different sub-domains according to the state of the solidification at the casting centreline: sub-domain I with liquid core ($f_s^{cent} = 0$), sub-domain II with non-strength core ($0 < f_s^{cent} \le f_s^{0-strength}$), and sub-domain III with 'rigid' core ($f_s^{cent} > f_s^{0-strength}$). In the sub-domain with liquid core, the whole solid phase moves with the solid shell, i.e. $u_x \equiv u_x^{Surf}$. In the sub-domain with 'rigid' core (no bulging in this region for Case II and Case III), we set u_x=0 which reflexes the symmetry condition. In the sub-domain with non-strength core (sub-domain I and II), it is distinguished between regions A and B. In region A, the strand thickens due to bulging, $u_x \equiv u_x^{Surf}$. In region B where the strand is pressed together, u_x decreases with decreasing solid fraction f_s from u_x^{Surf} at the 0-strength line ($f_s^{0-strength}$) to zero at the casting centreline [19] according to Equation (2).

Results

Case I: Macrosegregation with feeding flow. To gain information about the effect of shrinkage and bulging on the centreline macrosegregation in continuous slab casting of steel, a 2D symmetric benchmark steel (Fe-0.18 wt.% C) slab, 9000 mm length and 215 mm thickness, was simulated [19]. In Case I feeding flow induced by solidification shrinkage is the only mechanism causing interdendritic flow. Here, no gravity or bulging effects are considered. As schematically shown in Figure 2, the slab is assumed to be cast horizontally. The hot melt ($T_0 = 1791$ K) with nominal concentration ($c_0 = 0.18$ wt.% C) comes through the inlet (left), and the solid strand is continuously withdrawn from the outlet (right) with the casting velocity (u_z equals to casting speed of 6 mm/s). The heat transfer coefficient for the surface cooling ($T_w = 325$ K) is chosen to be 235 W/m^2 K. These boundary conditions are applied to achieve 'full' solidification within the calculation domain, when steady-state is reached. To simulate feeding, the liquid had a constant density of $\rho_\ell = 7027$ kg/m^3 and the solid of $\rho_s = 7324$ kg/m^3. To avoid feeding difficulties beyond a critical volume fraction of columnar $f_{s,SPM} = 0.95$ the so-called simplified porosity model (SPM) model [18, 19] is applied: Beyond 0.95 of solid volume fraction the remaining melt is supposed to solidify with the same density as that of the liquid melt. Thus, no feeding is necessary for solidification of the last 0.05 volume fraction of melt.

Figure 4 displays the observed macrosegregation profiles along the strand after reaching steady state. As already studied previously [19], positive segregation at the surface and negative segregation in the casting centre are predicted. These modelling results agree with previous studies [9, 11],

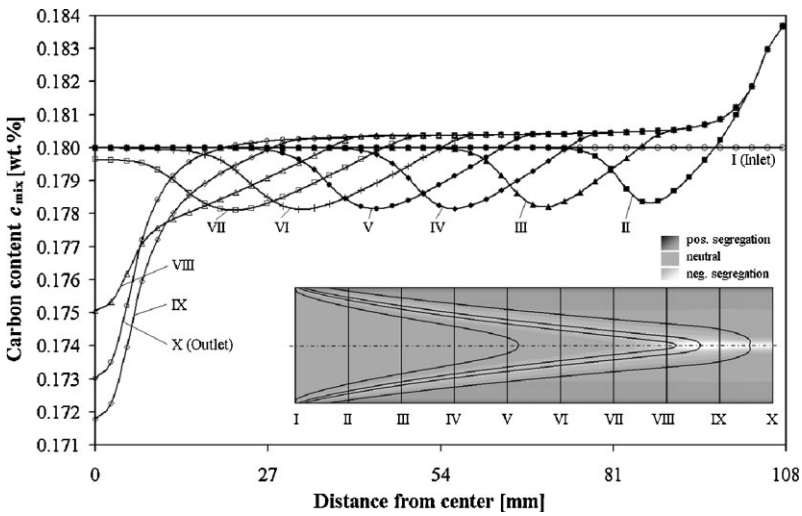

Figure 4. Predicted macrosegregation in a horizontal steel slab without bulging (length scaled 1:10). The evolution of macrosegregation along the casting direction is shown in terms of c_{mix}-profiles across the half of the casting. The position of each section (from I to X) is indicated in the lower figure displaying the c_{mix} distribution of the whole calculation domain. The four isolines in the insert show the solid volume fraction f_s of 0, 0.5, 0.8 and 0.95.

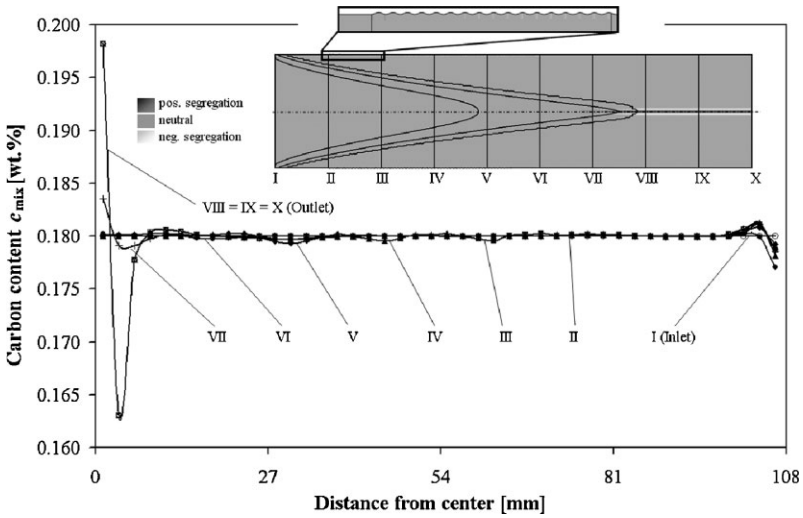

Figure 5. Predicted macrosegregation in a horizontal steel slab taking only bulging into account (length scaled 1:10). Figure details similar as in Figure 4, except the isolines in the insert show now the solid volume fraction f_s of 0, 0.5 and 0.8.

although they do not agree with industrial practice where mainly positive centreline segregation in the steel slab is observed. This indicates that the case which only considers shrinkage flow is different from reality.

Case II: Macrosegregation with bulging. Case II used the same boundary conditions as described for Case I. However, the geometry was changed from a rectangular one to a bulged one with $\delta_0 = 0.8$ mm and $N = 101$ rolls (Figure 2). δ_0 is the maximum of the displacement of the bulging, which occurs between the first pair of rolls. The displacement between the subsequent roll-pairs, δ, is linearly reduced. Since this case considers just bulging, the densities of the two phases are set to be equal, namely $\rho_\ell = \rho_s = 7027\,\mathrm{kg/m^3}$. The macrosegregation distribution as shown in **Figure 5** predicts positive centreline segregation which is gradually formed in the sub-domain II. Here, the dendrites in the mush below $f_s^{0-\mathrm{strength}}$ are deformed/ squeezed in region B according to the solid velocity field mentioned in Equation (2). Thus the segregated melt is pressed out of this region into region A and moves towards the casting centre.

Note, that the slightly segregated region adjacent to the casting surface in Figure 5 is a numerical artefact. It is anticipated that it is caused by an inaccurate interpolation of the bulging surface profile which artificially results in relative velocities between the liquid and solid phases. Here, further improvement of the numerical procedure is necessary. A further point worth mentioning is that for the present case of bulging the numerical calculation of the interdendritic flow in the high solid fraction region becomes much more difficult. Therefore, the solidification and the solidification shrinkage beyond the $f_{s,SPM}$ limit is ignored. With this simplification the metallurgical length (the position of end solidification), which corresponds now to a solid volume fraction of $f_s = 0.8$ (Fig. 5), is predicted to be shorter than in the last case (Fig. 4).

Case III: Macrosegregation with bulging and feeding. Case III uses the same boundary conditions as described for Case I and II. But this time, the bulged geometry was used as described in Case II with feeding flow being switched on.

The corresponding macrosegregation distribution as shown in **Figure 6** predicts positive centreline macrosegregation accompanied by negative 'valleys'. At the surface slightly positive segregation is observed. The typical inverse surface macrosegregation as known for cases with feeding (Fig. 4) is not reproduced properly. Again, this is due to an inaccurate numerical representation of sinuidal surface geometry.

Discussion

To get a better understand of the formation of the centreline segregation the relative velocity field between the melt and the solid phase in the two-phase region is studied. **Figures 7a and 8a** show the flow patterns of the relative velocity, $\vec{u}_l - \vec{u}_s$, for the two different cases considered: one is with bulging only, the other is with the combination of bulging and shrinkage-induced flow. In order to aid in analysing the flow patterns the position of the rolls are also indicated with filled arrows. The periodic flow pattern is caused by the periodic motion of the solidified strand shell (up and down).

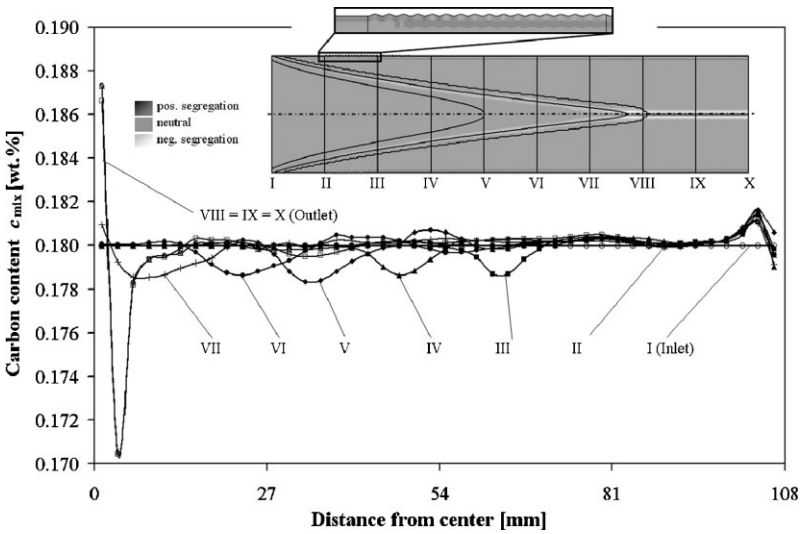

Figure 6. Predicted macrosegregation in a horizontal steel slab for bulging and feeding flow (length scaled 1:10). Figure details similar as in Figures 4 and 5.

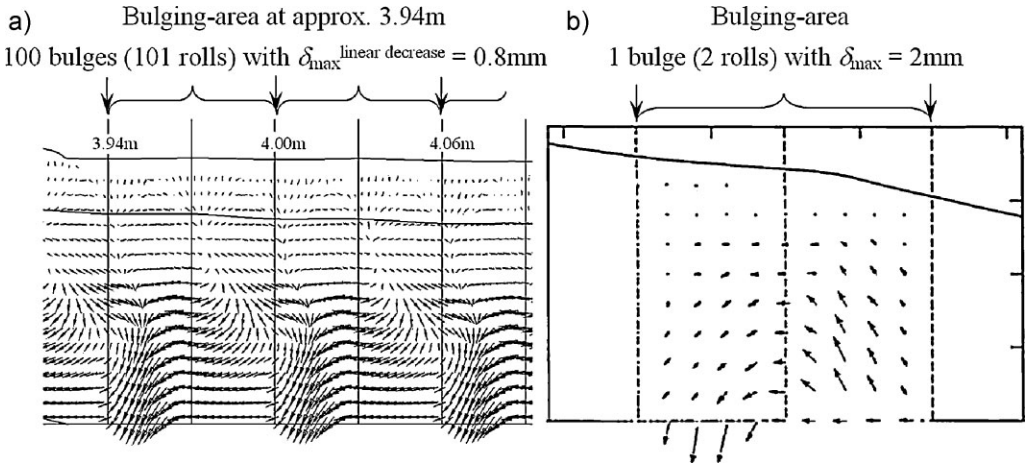

Figure 7. Comparison of the flow pattern obtained with a series of bulging (a) with a published result for only one bulging event [9] (b). Here only bulging is considered. For figure (a) the flow pattern is shown at approx. 3.94 m from the inlet. The positions of rolls are also indicated.

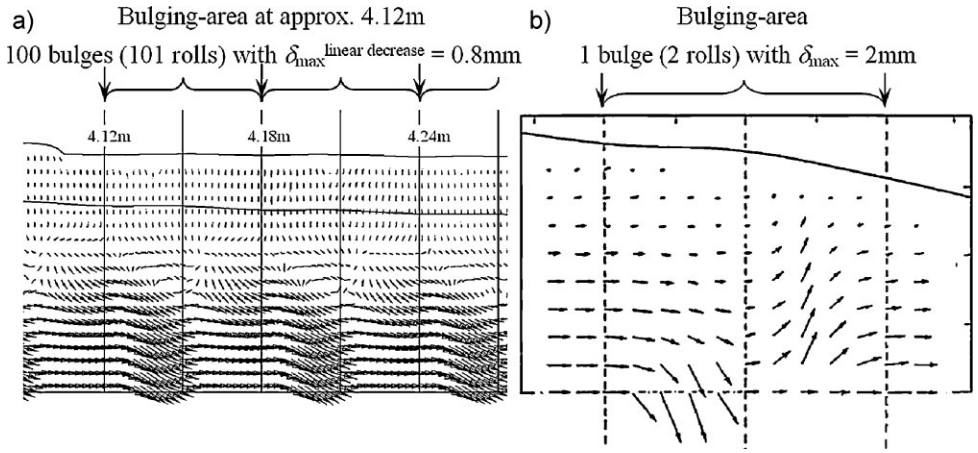

Figure 8. Comparison of the flow pattern obtained with a series of bulging (a) with a published result for only one bulging event [9] (b). Here both feeding and bulging-induced flow are considered. For figure (a) the flow pattern is shown at approx. 4.12 m from the inlet. The positions of the rolls are also indicated.

In the case of considering only bulging flow (no solidification shrinkage), Figure 7a, generally a negative relative flow field against the casting direction is observed. This is due to the fact that the average casting section is slightly reduced with the decrease of the bulging displacement. In the vertical direction, the up-down motion of the strand shell diverts the direction of the melt flow, up and down correspondingly. The details of the flow field depend on the position within the strand and might change remarkably. However, near the casting centreline the flow is diverted periodically towards the casting centre. This is the cause of the positive centreline macrosegregation.

In the case which considers both shrinkage and bulging-induced flow, Figure 8a, a relative velocity field parallel to the casting direction is predicted. The two flow mechanisms superimposed each other, but the feeding flow seems dominant. In the vertical direction, similar to the previous case (Fig. 7a), the up-down motion of the strand shell still diverts the direction of the melt flow, up and down correspondingly. Again, near the casting centreline, the flow is diverted periodically towards the casting centre. Therefore, a positive centreline macrosegregation occurs as well.

Both flow patterns predicted in the multiple bulging system (Figs. 7a, 8a) show qualitative good agreement with published results for cases which consider only a single bulging event (**Figure 7b**, **Figure 8b**) [9].

The z-component of the relative velocity, $u_{z,rel}$, along the casting centreline is plotted in **Figure 9**. The aforementioned three cases are compared. For the case considering only shrinkage-induced flow, Figure 9a, an acceleration and then deceleration of the relative velocity along the centreline can be seen. $u_{z,rel}$ is relatively large in comparison to the other cases, and it reaches its maximum ($\sim$1 mm/s) at a position of 66% of the metallurgical length. The reason for that is that the solid volume fraction of the centreline is low, and the melt takes the 'easiest way' to feed the solidification shrinkage in the downstream domain. The increase of $u_{z,rel}$ at

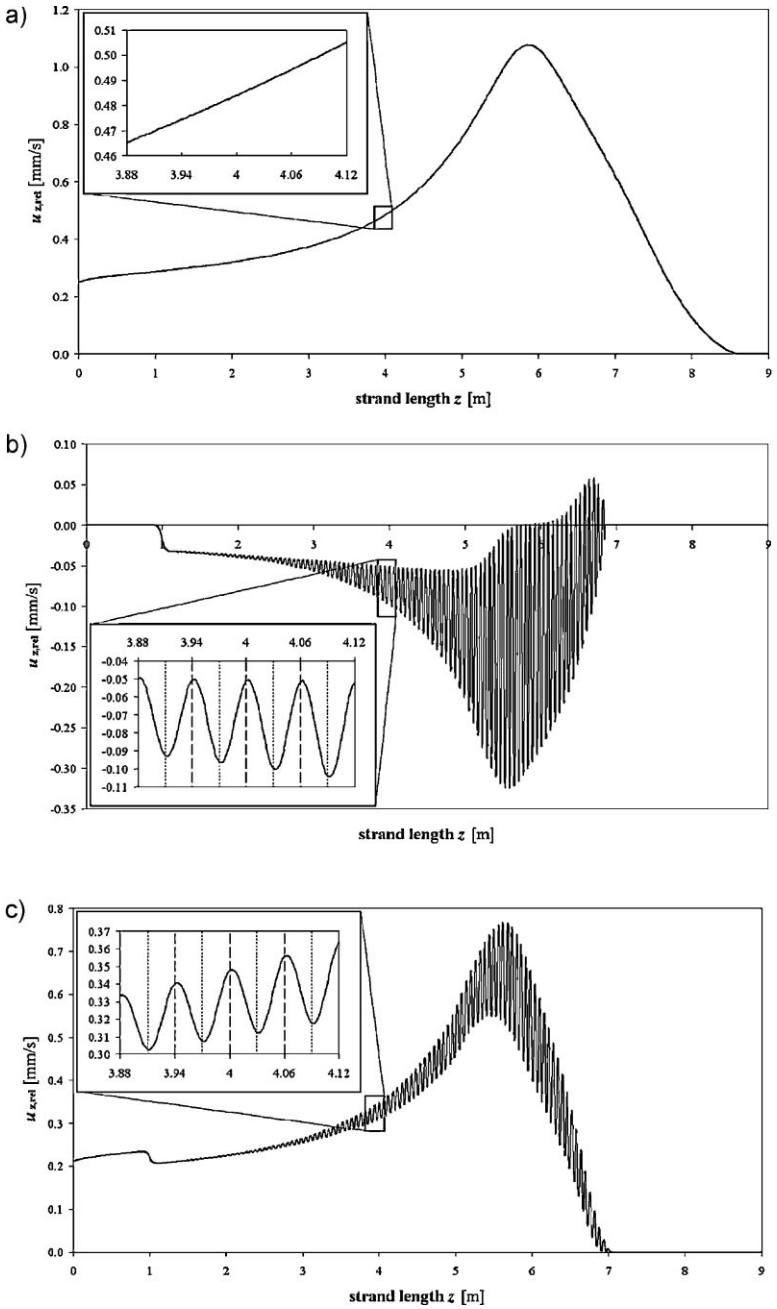

Figure 9. Distribution of the x-component of the liquid-solid relative velocity $u_{z,rel}$ along the casting centreline. (a) In the case of shrinkage (feeding) induced flow; (b) In the case of deformation (bulging) induced flow; (c) In the case of the combination of the shrinkage induced (feeding) and the deformation induced (bulging) flow.

the first 66% of the metallurgical length is mainly due to the fact that the flow channel becomes gradually narrow because of the progress of the solidification front towards casting centreline. The decrease of $u_{z,rel}$ after 66% of the metallurgical length is mainly due to the fact that the total volume in the downstream domain, which solidifies and needs to be fed, becomes smaller and smaller. Until the end of solidification at a position of about 8.5 m, no feeding is needed any more, and hence $u_{z,rel}$ tends to zero.

For the case of considering only bulging-induced flow, Figure 9b, the evolution of a non-zero $u_{z,rel}$ starts at the position where the first bulging roll is located (1 m), and ends at the metallurgical length which is in the present case just close behind the last bulging roll (at around 6.8 m). Note that in Case II and III the ''numerical'' metallurgical length is somewhat shorter then in Case I, as solidification (and thus solidification-induced feeding) is artificially switched off at $f_s = 0.8$ for Case II and III and at $f_s = 0.95$ for Case I. As mentioned earlier this was done to make convergence easier. Due to the sinusoidal profile of the bulged strand shell between the 100 roll-pairs, $u_{z,rel}$ oscillates correspondingly. This oscillating behaviour can be partially explained by Figure 7. A detailed analysis of the exact shape of this oscillating curve is beyond the scope of the present paper. However, it is obvious that in average a negative $u_{z,rel}$ is predicted along the centreline. This corresponds to the reduction of the bulging displacement δ. As no solidification shrinkage is considered, the reduction of δ results in a decrease of the casting cross section; hence the melt in the central liquid core is slightly pressed backwards. The backward velocity is relatively small ($\sim$ 0.05–0.3 mm/s).

When both shrinkage and bulging effects are coupled, Figure 9c, the model predicts that feeding flow generally dominates over the bulging-induced flow. A positive $u_{z,rel}$ is obtained, and in average it increases first, and then decreases as in Case I. However, the oscillating behaviour of $u_{z,rel}$ due to bulging is now overlaid. As previous results show, the final centreline segregation of the coupled shrinkage-bulging case (Fig. 6) is similar to the bulging-only case (Fig. 5), and different from the shrinkage-only case (Fig. 4). Again, it is obvious that it is the bulging-induced oscillating behaviour in the casting centreline that causes the positive centreline segregation, although the contribution of the oscillating behaviour to the overall $u_{z,rel}$ is rather small.

By comparing the obtained macrosegregation results with literature, it can be stated that the macrosegregation predicted by [9, 11] can be qualitatively confirmed by our simulation results for 101 bulging rolls. **Figure 10** shows the comparison of published results of macrosegregation profiles across the vertical section [9] with the macrosegregation profiles obtained in the current study, whereas **Figure 11** presents the comparison of macrosegregation profiles along the casting centreline obtained in the current study with published results [11]. Actually, the occurrence of macrosegregation is gradually strengthened through each pair of bulging rolls.

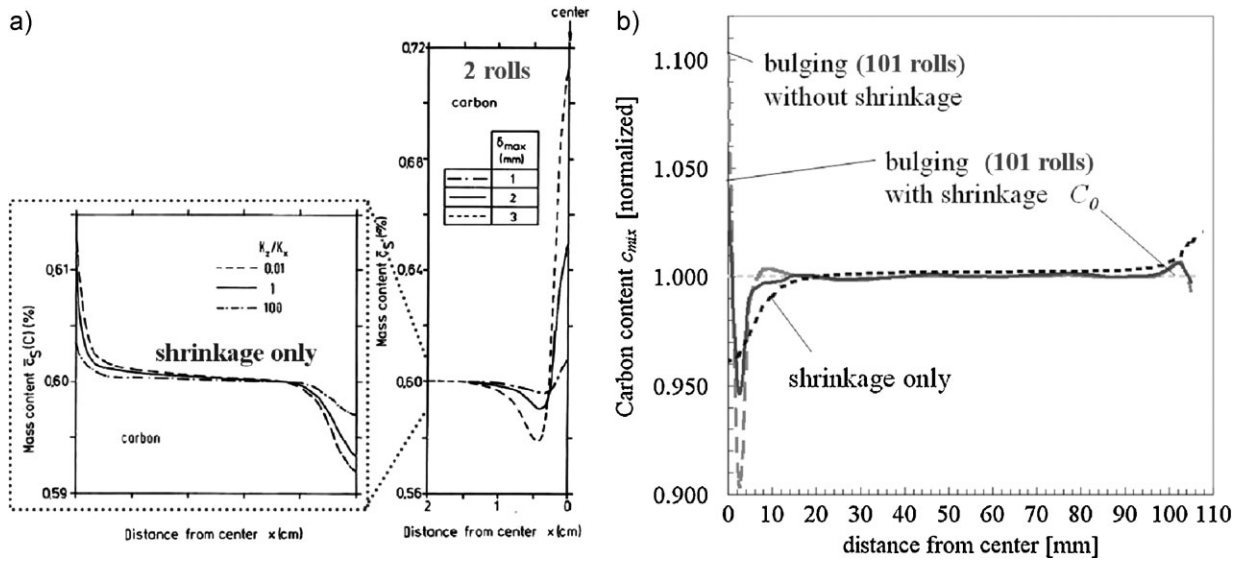

Figure 10. Comparison of published results of macrosegregation profiles across the vertical section [9] (a) with the macrosegregation profiles obtained in the current study (b). For the bulging geometry in our study we assumed $\delta_0 = 0.8$ mm and $N = 101$ rolls. Qualitatively, the predictions by the different authors agree with each other.

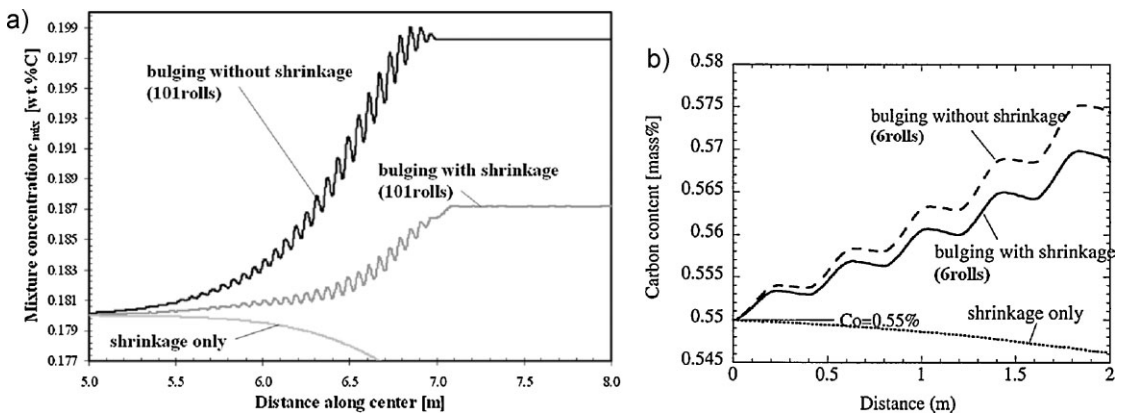

Figure 11. Comparison of the macrosegregation profiles along the casting centreline obtained in the current study (a) with published results [11] (b). It is obvious that the tendencies of the predictions of the two cases are consistent and that the effect of the bulging on the macrosegregation increases with increasing number of rolls.

The current results have demonstrated that the modelling idea of [9] with the use of an imposed solid velocity field allows to explain the positive centreline segregation which is accompanied by a negative segregation 'valley' as observed in industrial praxis. However, it would certainly be more precise to calculate the solid velocity rather than using predefined profiles. For the future development, incorporating the current multiphase solidification model into a thermal mechanical model as suggested by Bellet or Fachinotti [12, 13] would be desirable.

Conclusions

A two-phase volume averaging model was applied to study the shrinkage- and bulging-induced macrosegregation in continuous slab casting of steel. It is shown that considering only shrinkage-induced flow, the predicted macrosegregation pattern shows negative centreline segregation. Bulging of the solidified shell has a significant impact on the flow, especially in the interdendritic mushy region, and hence on the final macrosegregation formation which shows the opposite effect compared to the one caused by feeding. Here a pattern of positive centreline segregation accompanied by two negative minima is predicted with a series of bulging rolls. These modelling results agree with findings of previous studies [9, 11]. When the above two flow mechanisms are combined, bulging dominates over shrinkage, and so positive centreline segregation finally remains. The most significant finding gained from the present study is that the final result of the centreline

segregation in a continuously cast slab is the sum-up effect of the series of bulging reduced to some extent by solidification-induced feeding flow. With the help of the present model the impact of soft reduction on the formation of centreline segregation can now be investigated numerically. This will help to identify optimal process conditions for an effective reduction of detrimental macrosegregation close to the slab centre.

Acknowledgements

This work is financially supported by the Austrian Christian-Doppler Research Society, voestalpine Stahl Donawitz, voestalpine Stahl and Siemens VAI Metal Technologies for which the authors kindly acknowledge.

References

[1] S. Ogibayashi, M. Kobayashi, M. Yamada, T. Mukai: ISIJ Int., 31 (1991), 1400.
[2] C. H. Yin, J. K. Park, B. D. You, S. M. Yang: ISIJ Int., 36 (1996), 231.
[3] R. Thomas, K. Harste: Steel Res. Int., 75 (2004), 693.
[4] H. Preßlinger, S. Ilie, P. Reisinger, A. Schiefermüller, A. Pissenberger, E. Parteder, S. Bernhard: ISIJ Int., 46 (2006), 1845.
[5] O. Bode, K. Schwerdtfeger, H. G. Geck, F. Höfer: Ironmaking and Steelmaking, 35 (2008), 137.
[6] S. Ilie, R. Fuchs, K. Etzelsdorfer, C. Chimani, K. Mörwald: Proc. of 6th European Conference on Continuous Casting (2008).
[7] A. Kropf: Proc. of VAI Continuous Casting and Hot-Rolling Conference (2004) Paper 2.3.
[8] S. Ilie, H. Preßlinger, A. Schiefermüller, A. Pissenberger, P. Reisinger: BHM, 172 (2007), 227.
[9] K. Miyazawa, K. Schwerdtfeger: Archiv Eisenhüttenwesen, 52 (1981), 415.
[10] S. Y. Lee, A. I. Chung, A. P. Hong: Modeling of Casting, Welding and Advanced Solidification Processes IX, ed. P. Sahm, P.N. Hansen, G. Conley (2000), p. 648.
[11] T. Kajitani, J.-M. Drezet, M. Rappaz: Met. Mater. Trans., 32A (2001), 1479.
[12] M. Bellet, V. D. Fachinotti: Modeling of Casting, Welding and Advanced Solidification Processes XI, ed. C-A. Gandin and M. Bellet (2006), p. 168.
[13] V. D. Fachinotti, S. L. Corre, N. Triolet, M. Bobadilla, M. Bellet: Int. J. Numer. Meth. Engng., 67 (2006), 1341.
[14] A. Ludwig, M. Wu: Mater. Sci. Eng. A, 413–414 (2005), 109.
[15] M. Wu, A. Ludwig: Metall. Mater. Trans., 37A (2006), 1613.
[16] M. Wu, A. Ludwig: Metall. Mater. Trans., 38A (2007), 1465.
[17] R. B. Bird, W. E. Steward, E. N. Lightfoot: Transport Phenomena, New York, NY, John Wiley & Sons, 1960.
[18] F. Mayer, M. Grasser, L. Könözsy, M. Wu, A. Ludwig: 2nd Int. Conf. Modeling of Steelmaking, eds. A. Ludwig (2007), p. 265.
[19] F. Mayer, M. Wu, A. Ludwig: Modeling of Casting, Welding and Advanced Solidification Processes XII, ed. S.L. Cockcroft, D.M. Maijer, (2009), p. 279.

